*J. Physiol.* (1978), **275**, *pp.* 283–301
*With* 10 *text-figures*
*Printed in Great Britain*



# AFTERHYPERPOLARIZATION MECHANISM IN THE DORSAL SPINOCEREBELLAR TRACT CELLS OF THE CAT

BY B. GUSTAFSSON, S. LINDSTRÖM AND M. TAKATA*
*From the Department of Physiology, University of Göteborg, Göteborg, Sweden*

(*Received 30 March 1977*)

SUMMARY

1. The longlasting afterhyperpolarization (a.h.p.) following single or short trains of spikes in dorsal spinocerebellar tract (DSCT) neurones of the cat has been studied with intracellular recording techniques.

2. The a.h.p. amplitude was found to be potential dependent, increasing with depolarization and decreasing with hyperpolarization of the membrane. With large membrane hyperpolarization, the a.h.p. could be reversed in direction, the estimated reversal level being around 30 mV more negative than the threshold potential for spike initiation. The a.h.p. amplitude was also little affected by $Cl^-$ ions injected into the cell.

3. The a.h.p. was associated with an increase in the membrane conductance, as measured with short current pulses. The major part of the conductance change was related to the a.h.p. itself and not secondary to the hyperpolarization, i.e. to an anomalous rectification. A conductance change was also found when the membrane potential was polarized close to the a.h.p. reversal level. There was a clear correlation between the a.h.p. amplitude and the measured conductance changes.

4. It is concluded that the a.h.p. in DSCT neurones, as in spinal motoneurones, is caused primarily by an increase in membrane conductance to potassium ions.

5. The time course of the conductance change underlying the a.h.p. was calculated from the a.h.p. voltage and a mathematical expression describing this time course is given. The properties of the a.h.p. in DSCT cells are compared with those in spinal motoneurones and the functional significance of the differences is discussed briefly.

## INTRODUCTION

The soma-dendritic spike in many vertebrate neurones is followed by a longlasting afterhyperpolarization (a.h.p.). There is now much evidence that this a.h.p. is a major factor in the regulation of firing of the neurones, i.e. the neuronal mechanism governing the conversion of a synaptic input to an action potential output of a certain frequency (Kernell, 1965; Kernell & Sjöholm, 1973; Baldissera & Gustafsson, 1974*b*, *c*). In cat lumbar motoneurones the afterhyperpolarization is generated by a longlasting increase in the membrane permeability to potassium ions (Coombs, Eccles & Fatt, 1955) and recent observations indicate that this increase in potassium conductance is triggered by $Ca^{2+}$ ions which enter the cell during the action potential

* Present address: Department of Physiology, Dental School, Osaka University, 32 Joan-Cho, Kutaku, Osaka, Japan.

(Krnjević, Puil & Werman, 1975; Barret & Barret, 1976). Findings from other vertebrate neurones are compatible with a potassium mechanism for the a.h.p. (Takahashi, 1965; Baker & Precht, 1972). However, for the dorsal spinocerebellar tract (DSCT) cells the experimental observations have been interpreted to indicate that a sodium conductance process (Eide, Fedina, Jansen, Lundberg & Vyklický, 1969) or an electrogenic sodium pump (Kuno, Miyahara & Weakly, 1970) underlies the generation of the a.h.p. The possibility of a different a.h.p. mechanism in DSCT neurones is of interest, since the latter differ from motoneurones in being not 'integrating' neurones but 'relay' cells, interposed between primary afferents and cerebellum. Therefore, we have now reinvestigated the a.h.p. properties of DSCT neurones. It will be demonstrated that the a.h.p. in DSCT neurones is also caused by an increase in membrane conductance to potassium ions. In two subsequent papers the interaction between the a.h.p.s of successive spikes and the role of the a.h.p. in the regulation of repetitive firing in DSCT neurones will be considered (Gustafsson & Zangger, 1978; Gustafsson, Lindström & Zangger, 1978). Short preliminary reports of the present findings have been published (Gustafsson, Lindström & Takata, 1971; Gustafsson, 1974).

## METHODS

The experimental results presented in this and two consecutive papers (Gustafsson & Zangger, 1978; Gustafsson *et al.* 1978) have been obtained from thirty three adult cats. The animals were dissected under ether anaesthesia and during the recording sessions they were anaesthetized with pentobarbitone (Nembutal, Abbot; initial dose 25–30 mg/kg) or chloralose (60 mg/kg). Laminectomies were performed in the lower thoracic region and in the lumbar region (L2–L4). In nineteen experiments the anterior cerebellum was exposed by posterior occipital lobectomy and partial removal of the bony tentorium. In these experiments the DSCT cells were identified by antidromic activation from the cerebellum, the dorsal column and the contralateral half of the spinal cord being transected in the lower thoracic region. In the remaining experiments the cerebellum was not exposed but the DSCT cells were identified by antidromic activation from the dorsal quadrant of the ipsilateral lateral funicle dissected in the lower thoracic region and mounted for stimulation. The animals were immobilized with gallamine triethiodide (Flaxedil, May and Baker Ltd.) and artificially respired. Bilateral pneumothorax was performed to reduce respiratory movements. End tidal $CO_2$ was monitored with a Beckman medical gas analyser and kept within 4·5–5·5%. Rectal temperature was maintained at 37–38 °C; arterial blood pressure was continuously monitored throughout the experiments.

Intracellular recordings were made using electrodes filled with 2 M-potassium citrate or 3 M-potassium chloride, with the tips broken to 1·0–1·5 $\mu$m and with a DC resistance of 5–10 M$\Omega$ measured in saline. In all experiments the micro-electrodes were inserted through the dorsal column. To avoid venous obstruction only a small hole was made in the dura, where the electrode was to be inserted (see Eide *et al.* 1969). The recorded potentials were fed via a cathode follower to a modified Tektronix 502 oscillograph having two pairs of beams with independent time bases. The input conductance was measured by injecting constant current pulses through the recording micro-electrode. The device used allowed compensation of the voltage drop across the micro-electrode resistance (Eide, 1968).

The investigation reported in this and the two following papers is based on data from more than 100 DSCT cells. As earlier reported (e.g. Eide *et al.* 1969) the DSCT neurones are easily injured by the micro-electrode penetration. In some cells the injury discharge settles down and by the application of steady hyperpolarizing current the spike activity can be controlled. In the cells selected for analysis a subthreshold membrane potential level could be maintained with injection of a steady hyperpolarizing current of 0–20 nA, usually around 10 nA. In this condition all cells gave spike potentials above 60 mV, the majority between 70 and 90 mV. The membrane potential level obtained by this procedure is referred to in the text as the 'holding potential' and was usually 5–15 mV below the threshold level for spike initiation. No attempt was made

to estimate the absolute membrane potential level since in our experience such estimates are very unreliable when the recording electrode is used for current injection. However, our holding potential presumably did not deviate more than 5–10 mV from the original resting potential.

The soma-dendritic spikes were evoked by antidromic activation from the cerebellum or ipsilateral dorsal quadrant of the spinal cord (see above). Precautions were taken to ascertain that the studied spike afterpotentials were caused by the soma-dendritic spikes themselves and not due to descending or recurrent synaptic effects. The spikes were evoked at just suprathreshold intensity for each individual cell after having first confirmed that there were no detectable synaptic potentials following stimuli straddling the threshold, and that the spike afterpotentials at threshold and just suprathreshold strengths were identical. With repetitive activation of the ipsilateral dorsal quadrant synaptic potentials were sometimes observed, and in such cases the spikes were instead evoked by short (< 1 msec) intracellular current pulses. These procedures do not exclude recurrent synaptic effects from the axon of the impaled cell. Such recurrent effects have, however, never been observed so far (Kuno & Miyahara, 1968; Lindström, S., unpublished). Moreover, in several cells the membrane was depolarized or hyperpolarized so as to block the soma-dendritic invasion of the spikes, without revealing any hidden synaptic effects.

In the computation described in section V the voltage and duration values were supplied to eqn (1) by analogue–digital conversion using a Hewlett–Packard digitizer (9864A). This procedure allowed a resolution of 0·02–0·05 mV in the a.h.p. amplitude and a time resolution of 0·1–0·4 msec. Calculations were made by a Hewlett–Packard calculator 9830A and the results directly plotted by a Hewlett–Packard calculator plotter 9862A.

## RESULTS

The typical sequence of afterpotentials following an action potential in a DSCT neurone is illustrated in Fig. 1*A*. The falling phase of the action potential ends in a hyperpolarizing undershoot (double arrow; second trace). The undershoot is followed by a rapid repolarization which sometimes exceeds the resting membrane potential level, giving rise to a delayed depolarization (single arrow, both traces). This repolarization is interrupted and followed by a later hyperpolarization, the a.h.p., which has a duration of 30–120 msec (Kuno & Miyahara, 1968; Eide *et al.* 1969). As shown by the absence of these potential changes in one of the superimposed traces, where the spike invasion failed, these afterpotentials are generated by the action potential and are not due to synaptic activity (see also Methods).

### *I. Potential dependence of the a.h.p.*

It was reported by Eide *et al.* (1969) that in DSCT cells the a.h.p. following a single spike diminished considerably with rather weak hyperpolarization of the membrane, disappearing before the membrane potential had reached a presumed potassium equilibrium potential. On the other hand, it was later claimed by Kuno *et al.* (1970) that the a.h.p. following single as well as a train of spikes was practically independent of the membrane potential level, despite potential displacements beyond a presumed potassium equilibrium potential.

In the present experiments the effect of membrane potential displacements on the a.h.p. was studied, either by giving polarizing constant current pulses of various strength and direction or by changing the amount of steady polarizing current injected into the cells from the recording micro-electrode. Records from such experiments are illustrated in Figs. 1–3 and the results are representative for the thirty neurones in which the potential dependence of the a.h.p. was tested. It can be seen that the a.h.p. following a single (Fig. 1*C*) as well as a short train of spikes (Fig. 2*A*) is dependent on the membrane potential level, decreasing with hyperpolarization

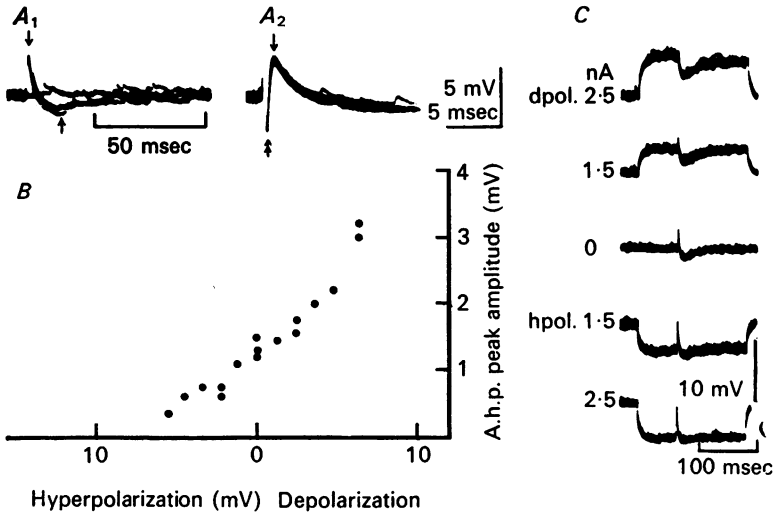


Fig. 1. Membrane potential dependence of the afterhyperpolarization (a.h.p.) following a single spike in a DSCT neurone. $A_1$, afterpotentials following a single spike evoked by stimulation of the cerebellar cortex, upward arrow denotes the a.h.p. peak, downward arrow the peak of the delayed depolarization. $A_2$, expanded record of $A_1$; double arrow indicates the peak of the initial undershoot; in this and subsequent records several (five–ten) sweeps are superimposed. *B*, plot of the a.h.p. peak amplitude against membrane potential displacement from the holding potential (0 mV in the graph; steady hyperpolarizing current 10 nA). *C*, some of the records used for the plot in *B*; observe the increase in the a.h.p. amplitude with depolarization (dpol.) and decrease with hyperpolarization (hpol.) from the holding potential.

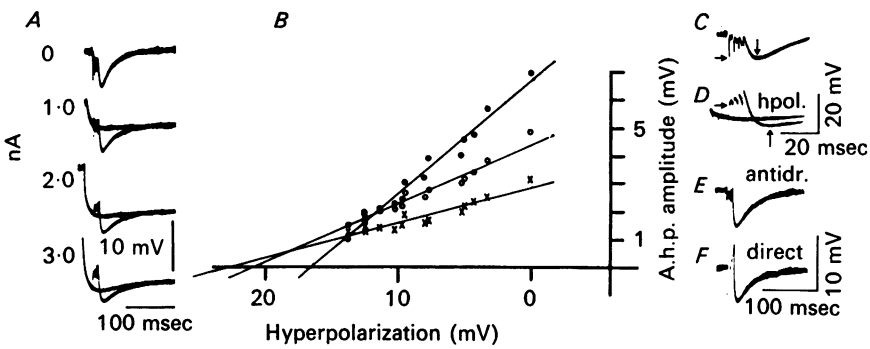


Fig. 2. Membrane potential dependence of the a.h.p. following a short train of spikes. *A*, A.h.p. given by five antidromic spikes evoked by cerebellar stimulation at a frequency of 400/sec; steady hyperpolarizing current 1 nA; sample from series of records used in the plot in *B*. Observe the decrease in the a.h.p. amplitude when superimposed on hyperpolarizing current pulses. *B*. Plot of the decrease in the a.h.p. amplitude with increasing hyperpolarization as illustrated in *A*; ●, 7·5 msec, ○, 20 msec and ×, 30 msec, after the last spike in the train. *C*, a.h.p. evoked at the holding potential. *D*, a.h.p. evoked during a 3·5 nA hyperpolarizing pulse. Vertical arrows in *C* and *D* denote the a.h.p. peak. Horizontal arrows denote the peak of the brief undershoot. Observe in *D* the 'reversal' of the undershoot with respect to the baseline. *E*, afterpotential following a train of spikes evoked by antidromic activation from cerebellum. *F*, afterpotential following a train of spikes directly evoked by a current pulse injected into the neurone (same number of spikes as in *E* at a similar frequency). Note the similar amplitude and shape of the a.h.p. in *E* and *F*.

and increasing with depolarization of the membrane. The effect of large hyperpolarizations of the membrane was difficult to study, partly due to blockage of soma-dendritic invasion of the spike, and partly due to the anomalous rectification of the cell membrane (see below), which made large current injections necessary. However, in two neurones where large steady hyperpolarizing currents were applied, the a.h.p. not only decreased with hyperpolarization but reversed in direction so that the spikes were followed by a longlasting depolarization (Fig. 3*A*). By application of a hyperpolarizing current pulse immediately after the last spike in the train,

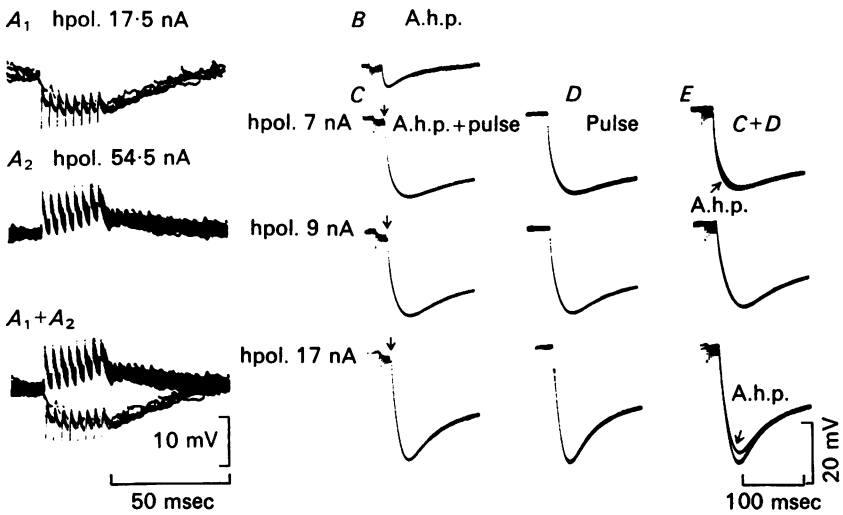


Fig. 3. Reversal of the a.h.p. with membrane hyperpolarization. $A_1$, a.h.p. following a short train of spikes at the holding potential (steady current 17·5 nA); antidromic activation from the cerebellar cortex. $A_2$, spikes evoked during a 54·5 nA steady hyperpolarization (hpol.) current. $A_1+A_2$, superimposition of $A_1$ and $A_2$; observe that the postspike depolarization in $A_2$ lasts as long as the a.h.p. in $A_1$. *B*, another DSCT cell; a.h.p. following a short train of spikes evoked by stimulation of the cerebellar cortex at a frequency of 400/sec (steady current 1 nA). *C*, current pulses (7, 9 and 17 nA) given just after the last spike in the train. *D*, current pulses alone. *E*, superimposition of the records in *C* and *D*; the difference between the two traces in *E* shows the post-spike potential; note the change from a hyperpolarizing post-spike potential at 7 nA (arrow) to a depolarizing potential at 17 nA (arrow), i.e. the reversal of the a.h.p. (for further details, see text).

in order to avoid blockage of soma-dendritic invasion (Coombs *et al.* 1955), a similar reversal was observed in two additional neurones (Fig. 3*B–E*). In these two cells the reversal potentials were estimated to be 27 and 22 mV more negative than the holding potentials which in turn were respectively 5 and 10 mV more negative than the threshold potential for spike initiation. These measurements should be interpreted with some caution since the electrode resistance might have changed during the injection of the required large current pulses.

The reversal level for the a.h.p. was also estimated by plotting its amplitude against the membrane potential displacement induced by smaller hyperpolarizing current pulses. When the a.h.p. amplitude was measured at a constant interval from the spike onset (corresponding to the peak of the a.h.p. at the most depolarized

level), an approximately linear decay with hyperpolarization was found (closed circles in Figs. 1*B* and 2*B*). The extrapolated reversal levels were 7·5 mV (Fig. 1*B*) and 16·5 mV (Fig. 2*B*) below the holding potentials which were around 15 mV (Fig. 1*B*) and 5 mV (Fig. 2*B*) below the threshold level in these cells. Since the data in Figs. 2*B* and 3*B* were obtained from the same cell, it is clear that this extrapolation procedure gives a considerable underestimate of the a.h.p. reversal level (21·5 mV versus 32 mV below threshold). However, from the expanded records in Fig. 2*C* and *D* it can be noted that the time to peak of the a.h.p. is not constant over the potential range used but increases with hyperpolarization (arrows). This means that with increasing hyperpolarization the measurements are performed earlier and earlier during the descending phase of the a.h.p. and thus give underestimated values of the a.h.p. amplitude. As will be shown later (section VI), this change in the a.h.p. time course can be related to the increases in the delayed depolarization (with respect to the prespike potential) with hyperpolarization. The initial part of the a.h.p. current will thus be required to charge the membrane capacitance, thereby delaying the onset of the a.h.p. itself. To overcome this source of error the a.h.p. voltage could be measured later during the decay phase of the a.h.p. where the delayed depolarization influence is much less pronounced (cf. Fig. 10). The result of such measurements of the a.h.p. amplitude 20 msec (○) and 30 msec (×) after the last spike in the train is shown for the cell in Fig. 2*B*. These plots also show an approximately linear decay of the a.h.p. amplitude with hyperpolarization, but the extrapolated reversal levels are now 20·5 mV (20 msec) and 22·5 mV (30 msec) below the holding potential. This is significantly more negative than the values in the first plot (●) and closer to the reversal level estimated in Fig. 3*B–E*. It should be pointed out that the a.h.p. reversals illustrated in Fig. 3 are true reversals and not caused by the passive decay from the delayed depolarization peak. First, the a.h.p. in Fig. 3*A* is reversed during 50 msec, which is more than thirty times the membrane time constant at that potential level (1·6 msec). Secondly, when applying the hyperpolarizing pulse after the last spike in the train (Fig. 3*B–E*) no increase of the delayed depolarization occurs.

Results similar to those illustrated in Fig. 2*B* were found in six other cells examined in this manner. The estimated reversal levels from these neurones were around 15–20 mV below the holding potential or 20–30 mV below the threshold level. Unfortunately, the estimation of the reversal level from extrapolation of curves measured late during the a.h.p. was not very accurate either. Besides the decreased sensitivity in the measurements given by the smaller and noisier a.h.p. voltage in its later phase, the curves were often found to be non-linear, the a.h.p. decreasing slower with increasing hyperpolarization. This non-linearity, which was most probably associated with the anomalous rectification (section III) found in these cells would thus also tend to give an underestimation of the reversal level upon extrapolation. Bearing all these difficulties in mind it is nevertheless clear from the above results that the a.h.p. in DSCT neurones is potential dependent, with a reversal level some 20–30 mV more negative than the spike threshold level. In this context, it should also be mentioned that the a.h.p. in DSCT neurones (as in motoneurones; Coombs *et al.* 1955) is unaffected by chloride ion injections large enough to reverse i.p.s.p.s.

*II. Conductance change during the a.h.p.*

In motoneurones it is possible to demonstrate an increase in conductance during the a.h.p. when tested by measuring the voltage drop produced by small constant current pulses injected into the cell (Ito & Oshima, 1962; Baldissera & Gustafsson, 1974*a*). Using this technique Eide *et al.* (1969) observed only minor conductance changes in DSCT neurones. Similarly, Kuno *et al.* (1970) found practically no conductance changes even after a short train of spikes when the a.h.p. is considerably larger than after a single spike.

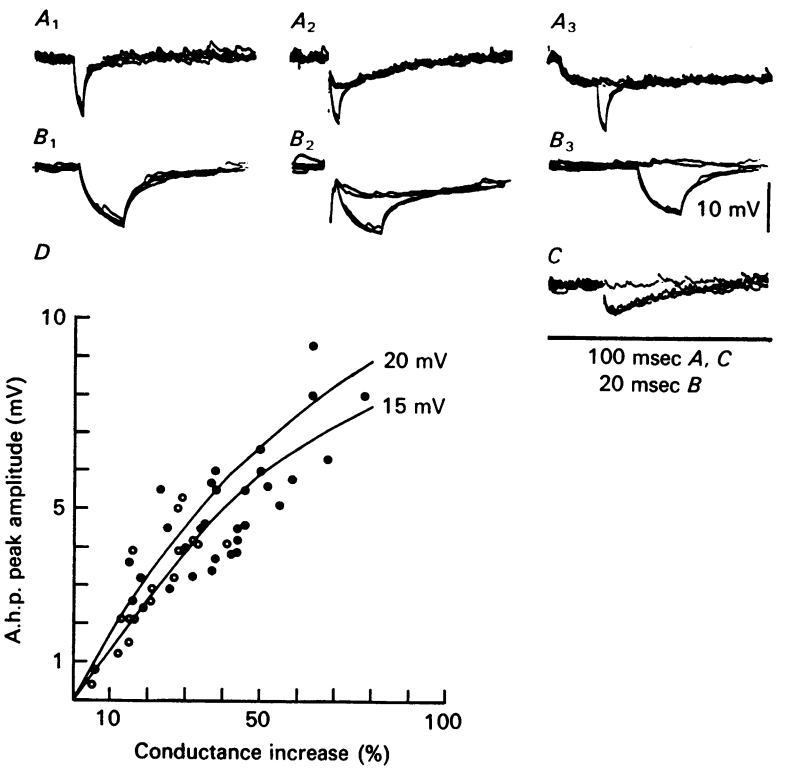


Fig. 4. Conductance change during the a.h.p. *A*, short constant current pulse (10 nA); alone ($A_1$); during the a.h.p. following an antidromic spike evoked from cerebellum ($A_2$) and during a long pulse giving the same hyperpolarization as the a.h.p. ($A_3$). $B_1$–$B_3$, expanded sweeps of $A_1$–$A_3$; note that the pulse amplitude is smaller when superimposed on the a.h.p. than at resting level and during the long pulse. *C*, a.h.p. following an antidromic spike, the stimulus straddling the threshold. *D*, plot of the a.h.p. peak amplitude against the percentage conductance change during the a.h.p.; the data were obtained from twenty-nine DSCT neurones; values from a.h.p. following single spikes (○) and short trains of 2–10 spikes (●). The two solid lines represent the theoretical relationships between the magnitude of the conductance change and the resulting steady voltage displacement. They are calculated from the expression $(V_{ahp} - V) \times G_{ahp} = G_L \times V$, where $V_{ahp}$ (15 and 20 mV) is the potential difference between the holding potential level and the equilibrium potential for the conductance process, $G_{aph}$ is the value of the conductance. $G_L$ is the resting conductance of the cell and $V$ is the voltage displacement given by the conductance process.

In this study conductance changes during the a.h.p. have been measured in twenty-nine DSCT neurones. In eighteen cells the conductance was measured close to the peak a.h.p. following a single spike and a typical result is illustrated in Fig. 4. It can be observed that the voltage drop produced by the current pulse is smaller when applied during the a.h.p. (Fig. 4 $A_2$, $B_2$) than when applied at resting level (Fig. 4 $A_1$, $B_1$) indicating a conductance increase during the a.h.p. (cf. Discussion). A similar change in conductance was observed in all the neurones tested, the conductance after a single spike being 5–50% larger than the resting conductance.

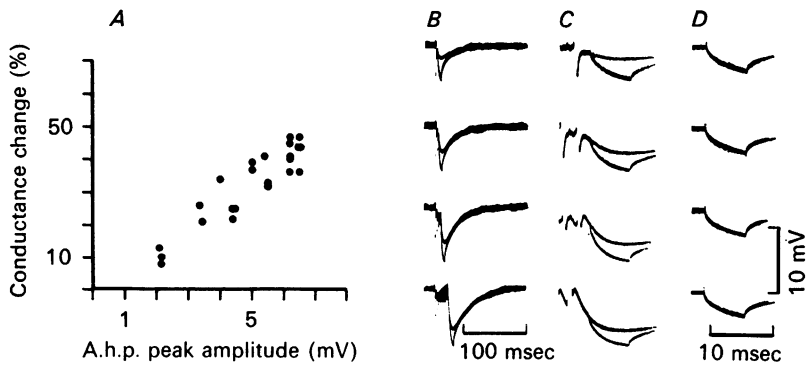


Fig. 5. Relation between a.h.p. peak amplitude and a.h.p. conductance change with increase in spike number. *A*, the a.h.p. peak amplitudes given by short trains of antidromic spikes (1–9) at 400/sec plotted against the percentage conductance change as measured with short current pulses. *B*, some records from the series used for the plot in *A*. *C*, expanded sweeps of *B*. *D*, test pulse alone at holding membrane potential: there was no significant anomalous rectification in this neurone.

When a train of spikes is evoked in DSCT neurones the a.h.p. amplitude increases with successive spikes, i.e. there is an a.h.p. summation (Eide *et al.* 1969; Kuno *et al.* 1970). In motoneurones, this summation is associated with an increase in the conductance change underlying the a.h.p. (Ito & Oshima, 1962; Baldissera & Gustafsson, 1974*c*). As illustrated in Fig. 5 the same results were obtained in DSCT cells. In this neurone the conductance change was measured at the a.h.p. peak after one to ten spikes (see sample records in Fig. 5, *B–D*). Fig. 5*A* shows that the increase in a.h.p. amplitude following several spikes is matched by a similar increase in the conductance during the a.h.p.

The conductance change during the a.h.p. was not secondary to the hyperpolarization itself. This was excluded, as shown in Fig. 4$A_3$, $B_3$, by applying the test pulse during another hyperpolarizing pulse of the same amplitude as the a.h.p. In this cell the voltage drop produced by the test pulse was somewhat less during the hyperpolarizing pulse (Fig. 4$A_3$) than at the holding potential (Fig. 4$A_1$). Such a decrease in membrane resistance with hyperpolarization, known as anomalous rectification (Nelson & Frank, 1967), was found in many DSCT neurones (see section III). However, in eight of ten neurones tested the conductance change given by the current induced hyperpolarization was one third or less of that during the a.h.p. of the same amplitude (*cf.* Fig. 4$A_2$, $A_3$). Thus is seems likely that the predominant

part of the conductance change measured during the a.h.p. is casually related to the a.h.p. mechanism.

The existence of anomalous rectification in many DSCT neurones, as well as the difficulty in determining precisely the a.h.p. reversal potential, made a more exact quantitative comparison between the measured increase in a.h.p. conductance and the a.h.p. amplitudes impossible. Another complicating factor was the need to use short test current pulses (5–10 msec), which did not allow the voltage drop to reach its final value. This means that the measured conductance changes were underestimated by 5–25% in different cells (see Fig. 2, Baldissera & Gustafsson, 1974*a*).

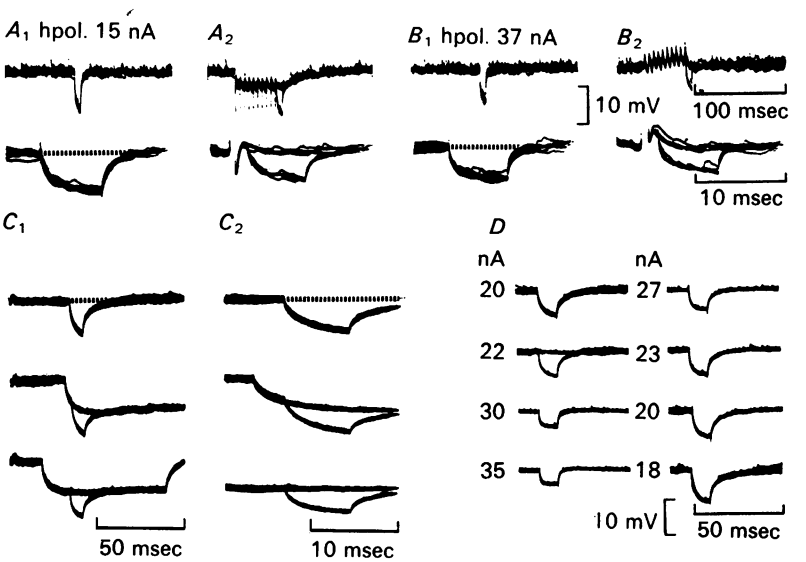


Fig. 6. Potential dependence of the a.h.p. conductance and the membrane conductance. *A*, current pulse (10 nA) applied alone ($A_1$) and during the a.h.p. following a short train of spikes ($A_2$) at the holding membrane potential (steady current 15 nA). *B*, same as in *A*, but at a membrane potential close to the a.h.p. reversal level (steady current 37 nA). Lower traces in *A* and *B* show the same pulses recorded with faster sweep speed. Interrupted lines denote the base line, i.e. the potential level without the pulse. Observe that the pulse in $B_2$ is smaller than in $B_1$ indicating a conductance change during the a.h.p., even close to its reversal level. *C*, development of anomalous rectification in another DSCT neurone. $C_1$, a short (5 nA) current pulse alone (upper trace), and superimposed at different intervals on a long (5 nA) current pulse (middle and lower traces). $C_2$, expanded records of the pulses in $C_1$; note that the short pulse is smaller when superimposed on the long pulse than at the resting level and that it has much the same amplitude when applied early during the hyperpolarizing phase of the long pulse as later on; voltage calibrations as in *B*. *D*, sequence of records with a short current pulse (5 nA) applied at different levels of steady membrane hyperpolarization from another DSCT cell; note the decrease in pulse amplitude when the hyperpolarizing current is increased from 20 nA to 35 nA and the subsequent recovery when the injected current is decreased.

Keeping these reservations in mind there was in all cells a clear correlation between the a.h.p. peak amplitude and magnitude of the measured conductance change during the a.h.p. This is apparent from Fig. 4*D*, whether a.h.p.s followed single or short trains of spikes. For comparison, the theoretical relation between the

magnitude of the conductance increase and the resulting steady state voltage change for a conductance process with an equilibrium potential 15 and 20 mV below the holding potential is also shown in Fig. 4*D*. Clearly the observed conductance changes can account for most, if not all, of the a.h.p. voltage amplitudes.

Due to the anomalous rectification in most neurones it was impossible to evaluate whether the a.h.p. conductance change varied with the membrane potential. However, Fig. 6*A–B* illustrates a cell which had only a slight anomalous rectification, where there was still a considerable increase in conductance during the a.h.p. when the membrane potential was polarized close to the reversal level of the a.h.p. (Fig. 6$B_1$, $B_2$). In fact the conductance change during the a.h.p. was much the same at this membrane potential level as at the original holding potential (cf. Fig. 6*A*, *B*). An increase in a.h.p. conductance at a membrane potential level close to a.h.p. reversal was found in two additional neurones. In another cell, lacking anomalous rectification, there was no significant alteration in the conductance change when the membrane potential was varied over a 15 mV range around the holding potential. These findings suggest that the conductance process underlying the a.h.p. has little voltage dependence in the potential range between the spike threshold and the a.h.p. reversal potential.

### *III. Anomalous rectification*

As in motoneurones (Nelson & Frank, 1967) the input resistance in many DSCT neurones was potential dependent, decreasing with hyperpolarization from the threshold level. This anomalous rectification was observed in thirteen of seventeen neurones tested. The membrane potential was displaced either with current pulses (ten cells) or by constant current injection (seven cells). Even when large steady hyperpolarizing currents were used, this decrease in input resistance was reversible when the amount of injected current was decreased (Fig. 6*D*). The anomalous rectification was very variable between cells. Of the cells tested with small current pulses, three cells were without significant rectification and four cells had a conductance change of less than 15% for a 5 mV membrane potential displacement in the region around the holding potential. However, in one cell a conductance change of 30% for a 5 mV displacement was observed.

In motoneurones the anomalous rectification has been claimed to develop with a slow time course (Nelson & Lux, 1970) and would thus not affect the conductance measurements obtained from the peak of the a.h.p. In two DSCT cells tested, the anomalous rectification developed almost instantaneously as seen in Fig. 6*C*. This quick inception of the rectification means that it has to be taken into account when the a.h.p. conductance is evaluated. However, as pointed out in section II the conductance increase caused by the hyperpolarization itself was always considerably less than that observed during the a.h.p. (cf. Fig. 4).

### *IV. A.h.p. amplitude*

The a.h.p. peak amplitude after a single spike was measured in fifty-eight neurones and varied between 0·8 and 6·2 mV (mean value 2·6 mV) with a distribution as shown in Fig. 7*A*. These values correspond well with those reported by Kuno and Miyahara (1968) (0–5 mV) but are larger than those given by Eide *et al.* (1969). The time from

the spike onset to the peak of the a.h.p. was measured in the same neurones and varied between 2·0 and 11·9 msec (mean value 6·8 msec) with a distribution as shown in Fig. 7*B*.

These a.h.p.s were measured at a holding potential 5–15 mV from the threshold for spike initiation, which would be about 15–20 mV positive to the a.h.p. reversal level (cf. section I). At this holding potential the initial hyperpolarizing undershoot

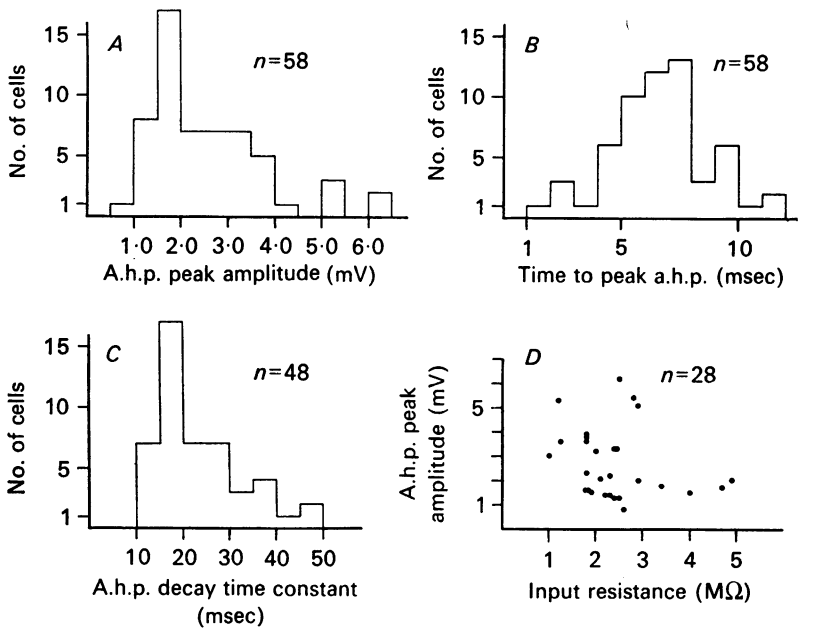


Fig. 7. A.h.p. parameters in DSCT cells. *A*, distribution of the a.h.p. peak amplitudes for fifty-eight neurones. *B*, distribution of the time to peak of the a.h.p. for the same neurones. *C*, distribution of the time constant for the repolarizing phase of the a.h.p. measured as discussed in the results. *D*, relation between the a.h.p. peak amplitude and the input resistance for twenty-eight neurones.

was between 5–10 mV. Ideally, these measurements should have been performed at potential levels equidistant from the a.h.p. reversal level. However, as indicated previously the reversal potential of the a.h.p. could not be determined very accurately. This means that the driving force for the a.h.p. varied somewhat between cells but this difference cannot account for the wide range in a.h.p. amplitudes (Fig. 7*A*). Neither were the differences in a.h.p. amplitudes due to differences in the input resistance of the neurones. As shown in Fig. 7*D* there was no tendency towards a smaller input resistance in cells with smaller a.h.p.

### *V. A.h.p. conductance time course*

The a.h.p. in DSCT cells, as in motoneurones, can have a duration of around 100 msec. Since the time constant of the DSCT cells was 2–10 msec (mean value 6·5, $n = 15$; see also Kuno & Miyahara, 1968) the a.h.p. decay cannot be accounted for by passive membrane properties. Thus a slowly decaying active process has to be considered to explain the long a.h.p. duration. In a few cells an attempt was made

to measure with small current pulses the time course of the conductance change underlying the a.h.p. The result from the best cell is shown in Fig. 8. The conductance increase was largest immediately after the spikes and decreased continuously thereafter during the hyperpolarization and subsequent repolarizing phase of the a.h.p. Qualitatively similar results were observed in the other neurones, but the scatter of the measurements did not permit any conclusion regarding the details of the underlying conductance change.

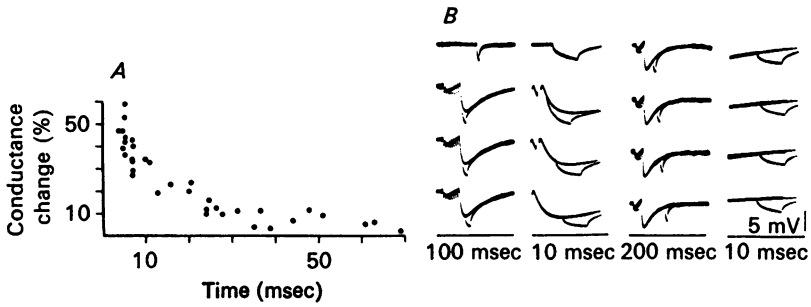


Fig. 8. Time course of the conductance change during the a.h.p. following a short train of spikes. *A*, plot of percentage conductance change against time after the onset of the last spike in the train. *B*, sample of records used for the plot in *A*.

On the assumption that the a.h.p. is caused by a single conductance process (an increase in the conductance for potassium ions, see Discussion) the time course of the underlying conductance change could be calculated from the a.h.p. voltage. To do this it has been assumed that the a.h.p. conductance is voltage independent in the potential range between the spike threshold and the a.h.p. reversal potential (see section II), that no other membrane parameters are changing during the a.h.p. and that the complex neuronal geometry can be neglected (cf. Baldissera & Gustafsson, 1974*a*). The conductance can then be computed from the voltage using this expression:

$$G_{\mathrm{ahp}}(t) = \frac{G_L \times V(t) + C \times \mathrm{d}V(t)/\mathrm{d}t}{V_{\mathrm{ahp}} - V(t)}, \tag{1}$$

where $G_{\mathrm{ahp}}$ = conductance underlying the a.h.p.;

$G_L$ = leakage or input conductance = 1/input resistance, calculated from the voltage drop caused by injection of constant current pulses;

$C$ = input capacitance = $\tau \times G_L$, where $\tau$ = membrane time constant (Rall, 1960);

$V_{\mathrm{ahp}}$ = difference (with a positive value) between the holding potential level and the a.h.p. equilibrium potential;

$V(t)$ = difference (with a positive value) between the holding potential level and the a.h.p. voltage.

This $G_{\mathrm{ahp}}(t)$ computation was performed in fifteen neurones throughout the spectrum of a.h.p. peak voltages and time to peaks given earlier. For each cell the values of $C$ and $G_L$ were determined and inserted into eqn. (1). The $V_{\mathrm{ahp}}$ value was, as discussed earlier, difficult to obtain and for these computations was set

arbitrarily at 20 mV. Changes of 5 mV around this value gave no changes in the computed time courses.

A typical result from such a computation is illustrated in Fig. 9. As in the time course measured with current pulses the conductance is largest initially at the peak of the delayed depolarization and decays continuously thereafter. In the very first part of the curve, the conductance makes a dip (see arrow), corresponding to the delayed depolarization. Since the delayed depolarization is a phenomenon separate

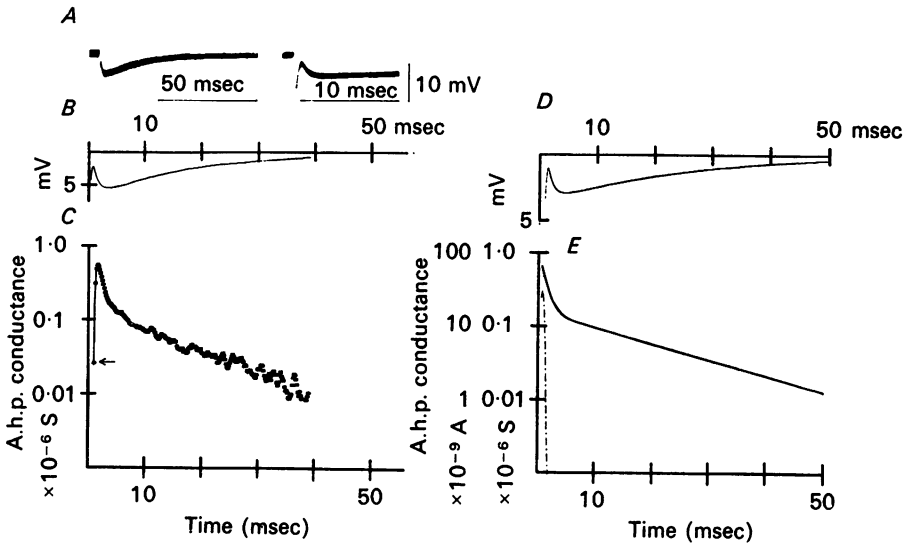


Fig. 9. Time course of the conductance change underlying the a.h.p. *A*, a.h.p. following an antidromic spike evoked by stimulation of the ipsilateral dorso-lateral funicle; steady current 10 nA; two different sweep speeds. *B*, a.h.p. in *A* plotted on a different scale. *C*, the calculated a.h.p. conductance plotted against time (logarithmic ordinate). Cell input resistance and capacitance were 2·6 MΩ and 2·7 nF respectively. The arrow indicates the initial dip in the calculated conductance related to the delayed depolarization. *D*, model a.h.p. calculated with the use of equation (5) in the text; starting values were 0·5 msec and 7·5 mV. *E*, model conductance time course given by equation (2) (solid line); interrupted line shows the time course of the delayed depolarization current using equation (4). The parameters used for the model computations in *D*, *E* are given in the text.

from the a.h.p. conductance, this part of the computed curve is considered an artifact. It will be noted that for the later part of the curve, the decay can, except for the initial phase, be approximated by a single straight line, implying an exponential decline of the conductance. A similar $G_{ahp}(t)$ shape was found in all the cells examined. In none of the cells was there any plateau or local minimum–maximum sequence as found with similar computations in motoneurones (Baldissera & Gustafsson, 1974*a*). The initial faster decay was present in all but two of the neurones examined and could also be relatively well approximated by a straight line. The time constant of this decay was very variable, from 1·1 to 6·6 msec with a mean value of 3·0 msec ($n$ = 13). Since this initial part of the a.h.p. is possibly influenced by geometrical factors as well as the delayed depolarization current, these values are purely descriptive and not intended to represent the exact shape of an underlying

conductance process (see Discussion). The time at which the two straight lines, approximating the initial and the later decay, intersected each other varied greatly, ranging from 3·9 to 8·3 msec with a mean value of 5·6 msec. To obtain a larger sample for the time constant of the slow $G_{ahp}(t)$ decay, the a.h.p. voltage, corrected for the change in driving force (Martin, 1955) was directly plotted against time on a logarithmic ordinate. This procedure was performed in thirty-three neurones, after single as well as after trains of spikes. The decay, thus estimated, was also approximated by a straight line, whose slope was rather unaffected by the number of spikes (Gustafsson & Zangger, 1978). The time constant of the slow $G_{ahp}(t)$ decay was thus measured in a total of forty-eight neurones and varied, as shown in Fig. 7*C*, between 10·0 and 48·7 msec (23·2 ± 9·7, S.D.).

*VI. Mathematical expression for a.h.p. conductance time course*

The conductance variation giving rise to the a.h.p. can be considered as a time dependent process, which follows a course with an initial fast decay succeeded by a slow exponential decline. The following eqn.:

$$G_{ahp}(t) = A_1 \times \exp\left(-\frac{t}{A_2}\right) + B_1 \times \exp\left(-\frac{t^{B_2}}{B_3}\right) \tag{2}$$

is a reduced version of that earlier used for motoneurones (Baldissera & Gustafsson, 1974*a*). When supplied with suitable parameters this expression gives a good fit to the computed a.h.p. conductance curves (compare Fig. 9*C* and *E*). If this expression is inserted in the differential equation:

$$G_{ahp}(t) \times (V_{ahp} - V(t)) - G_L \times V(t) - C \times \frac{dV(t)}{dt} = 0 \tag{3}$$

the a.h.p. voltage $V(t)$ resulting from this conductance time course can be computed. This model includes no expression for the rapid falling phase of the spike nor an expression for the process giving rise to the delayed depolarization. Since the rapid repolarization in DSCT neurones ends in an undershoot, the peak of which is not much affected by membrane potential displacements (Kuno *et al.* 1970; see however, Gustafsson & Zangger, 1978), that shortcoming is compensated for by starting the computation at this 'fixed' level. To account for the delayed depolarization the expression has been found convenient:

$$DD(t) = C_1 \times \exp\left(-\frac{t^{C_2}}{C_3}\right) \times t^{C_4}, \tag{4}$$

where $DD$ = delayed depolarization. When supplied with suitable parameters this expression simulates a large rapid depolarizing current injection (Fig. 9*E*, interrupted line), which can be inserted in eqn. (3) to give

$$G_{ahp}(t) \times (V_{ahp} - V(t)) - G_L \times V(t) - C \times \frac{dV(t)}{dt} - DD(t) = 0. \tag{5}$$

With the values $A_1 = 0{\cdot}16 \times 10^{-6}$ S, $A_2 = 20$ msec, $B_1 = 0{\cdot}75 \times 10^{-6}$ S, $B_2 = 1{\cdot}2$, $B_3 = 1{\cdot}4$ msec, $C_1 = 43 \times 10^{-9}$ A, $C_2 = 5$, $C_3 = 2$ msec, $C_4 = 1$, $V_{ahp} = 17{\cdot}5$ mV, $G_L = 0{\cdot}7 \times 10^{-6}$ S, $C = 2{\cdot}5 \times 10^{-9}$ F, eqn. (5) was solved and the resulting a.h.p. voltage is given in Fig. 9*D*. It will be noted that this a.h.p. is very similar to the real one, with an initial fast decay from the delayed depolarization, reaching a peak around 5 msec and thereafter a slow decay.

In this model is it implicitly assumed that the a.h.p. conductance time course is unaffected by the membrane potential. It was argued by Eide *et al.* (1969) that the a.h.p. rapidly decreased with rather small hyperpolarization of the membrane, thereafter being not much affected by further polarization. As shown in Fig. 2*C*, *D* the a.h.p. time course was also affected by polarization of the membrane, the time to peak a.h.p. increasing with hyperpolarization. As a result the estimated reversal level of the a.h.p. varied with the interval after the spike at which the a.h.p. voltage was measured, giving more negative extrapolated reversal levels with larger intervals.

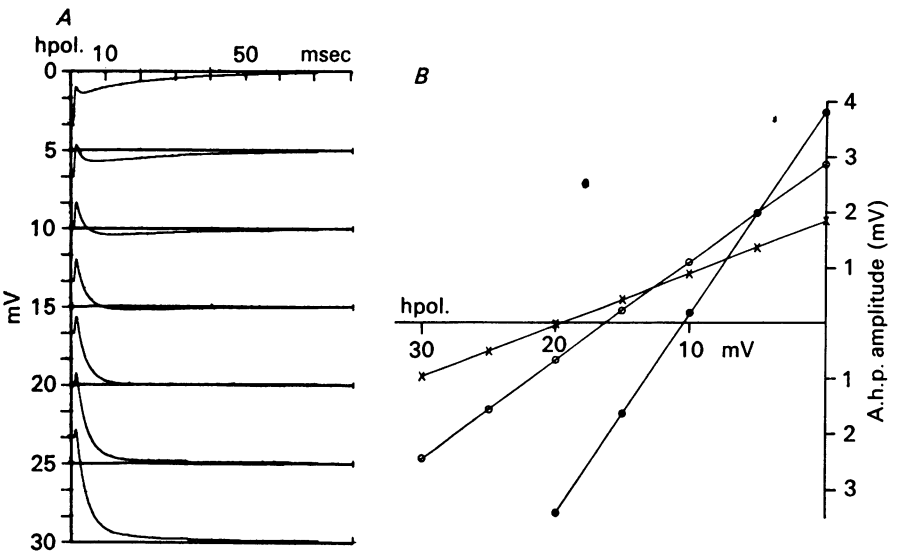


Fig. 10. Potential dependence of the model a.h.p. *A*, calculated voltage trajectories of the model a.h.p. in Fig. 9 at different membrane potential levels. The membrane potential was varied in 5 mV steps from a 'resting' level 20 mV less negative (upper trace) to a potential 10 mV more negative (lower trace) than the model a.h.p. equilibrium potential. *B*, plot of the model a.h.p. amplitude measured at 5 msec (filled circles), 10 msec (open circles) and 20 msec (crosses) after the 'spike onset' against the potential displacement from the 'resting level'. Note that the extrapolated 'reversal levels' for the 5 and 10 msec intervals are considerably less negative than the equilibrium potential used.

All these phenomena are easily reproduced by the model and should not be taken as indications for a potential dependence of the underlying conductance process. Fig. 10*A* shows the a.h.p.s resulting from computations performed at different potential levels, from resting level (0 mV) to the a.h.p. equilibrium potential (20m V) and beyond. With increasing hyperpolarization there is an increase in the time to peak a.h.p., as in real DSCT neurones, until the a.h.p. reaches its equilibrium potential (20 mV) and reverses (25–30 mV). This changing shape gives the appearance of a rapid initial reduction in a.h.p. amplitude with hyperpolarization (0–10 mV) followed by only small variations around the baseline (15–25 mV) (as observed for real neurones by Eide *et al.* 1969). The increase in time to peak of the model a.h.p. with hyperpolarization also leads to a shift in the estimated reversal level when the a.h.p. voltage is measured at longer intervals after the onset of the computations (cf. Figs. 10*B* and 2*B*).

## DISCUSSION

The present results suggest that the a.h.p. in DSCT neurones, as in spinal motoneurones, is caused by a permeability increase, probably to potassium ions. The a.h.p. is potential dependent with a reversal potential about 30 mV more negative than the threshold level for spike initiation and it is little affected by chloride ions injected into the cell. The a.h.p. is associated with a conductance increase, as measured with short current pulses. This conductance change is not secondary to the hyperpolarization, i.e. due to an anomalous rectification. As would be expected with a causal relationship between the conductance change and the a.h.p. mechanism there is a clear correlation between the measured conductance change and the a.h.p. amplitude in different cells.

It has been proposed earlier that the a.h.p. in DSCT cells is caused by a sodium conductance process (Eide *et al.* 1969) or an electrogenic sodium pump (Kuno *et al.* 1970). Eide *et al.* (1969) reported that the a.h.p. had a high sensitivity to polarizing current but they were unable to reverse it with hyperpolarization of the membrane. As shown by the a.h.p. computations in section VI their findings can be explained by the interaction of the delayed depolarization and the a.h.p. and the observations are thus fully compatible with the present results. The claim by Kuno *et al.* (1970) that the a.h.p. voltage is unaffected by membrane potential displacements seems to be caused by an insufficient hyperpolarization of the membrane (e.g. Fig. 5, Kuno *et al.* 1970) and by their procedure in measuring the a.h.p. amplitude (see Gustafsson *et al.* 1971). The fact that the a.h.p. polarizes the membrane to more negative values than the initial undershoot was taken as an additional evidence against a potassium conductance process underlying the a.h.p. (Kuno *et al.* 1970). This argument was based on the assumption that the peak of the undershoot is a measure of the potassium equilibrium potential, which is not the case (Gustafsson & Zangger, 1978).

No or only minor conductance changes during the a.h.p. were earlier reported (Eide *et al.* 1969; Kuno *et al.* 1970). The failures to detect significant conductance changes in these investigations might have been caused by an unawareness of the magnitude of conductance changes to be considered significant (see Gustafsson *et al.* 1971). The large temperature dependence of the half decay time of the a.h.p. in DSCT neurones ($Q_{10}$ = 2·4) was also held as an evidence for an electrogenic sodium pump (Kuno *et al.* 1970). However, this $Q_{10}$ value is very close to that found for a.h.p. in spinal motoneurones ($Q_{10}$ = 2·1, Klee, Pierau & Faber, 1974) and is thus not inconsistent with our suggestion that a potassium conductance increase underlies the a.h.p. in DSCT neurones.

It should be clear that most of the present observations on DSCT cells, as well as results from motoneurones, could be compatible with a sodium conductance decrease underlying the a.h.p. If it is assumed that the cell has a sodium conductance which is strongly voltage dependent, decreasing with membrane hyperpolarization, and if the spike reduces this sodium conductance, a potential dependent a.h.p. associated with a clear conductance change will result. In motoneurones, the participation of a sodium mechanism was negated since intracellular injection of sodium ions gave a decreased a.h.p. instead of a predicted increase (Coombs *et al.* 1955). However, if the

a.h.p. is caused by a sodium conductance decrease (or a potassium conductance increase) a decrease would in fact be predicted. The findings of an a.h.p. reversal and of a clear conductance increase during the a.h.p. when the cell membrane was polarized close to the a.h.p. reversal level excludes, however, a sodium conductance decrease as the primary cause of the a.h.p.

It was suggested by Eccles (1957) that the potassium conductance underlying the a.h.p. in cat spinal motoneurones was a separate conductance from the delayed rectification, i.e. the potassium conductance giving rise to the falling phase of the action potential. The presence of such a separation is supported by the finding of a selective depression of the a.h.p. found in some DSCT cells (Gustafsson & Zangger, 1974, 1978). More recently, two potassium conductances with different kinetics, one giving rise to the delayed rectification, the other to the a.h.p., have also been described in frog spinal motoneurones (Barret & Barret, 1976). From the present study we cannot decide to what extent the initial phase of the computed a.h.p. conductance is a mixture of delayed rectification and a.h.p. potassium conductance. In the frog spinal motoneurones the delayed rectification decays rapidly being virtually over at the peak of the delayed depolarization. If the same is true for DSCT neurones the whole computed conductance change would belong to the a.h.p. potassium conductance. The computed conductance was found to decay in two phases, an early fast and a later slow phase. As discussed in section V, this time course was derived from the a.h.p. voltage under the assumption that the geometry of the neurone could be neglected. This procedure would be correct only if the a.h.p. was evoked in such a large area of the cell that no a.h.p. current was drained from the soma out into the dendrites. If instead the a.h.p. was evoked only in the soma, there would be a difference between the real a.h.p. membrane conductance time course and the computed one. In this case the initial hyperpolarization would, as for a square current pulse (Rall, 1960), proceed faster than if the a.h.p. had been more equally distributed. When computed under the above assumption the conductance would then be overestimated in its initial part. Since the a.h.p. distribution is unknown it is not clear to what extent this factor is responsible for the two phase decay of the computed a.h.p. conductance.

On the assumption that the a.h.p. is the main factor regulating repetitive firing in DSCT neurones, the firing behaviour of such neurones could be simulated by a model based on their a.h.p. properties. For this reason a mathematical expression describing the calculated time course of the a.h.p. conductance was derived and given in section VI. It should be noted that this time course was calculated neglecting the influence of the geometry of the neurone (see above). When computing the repetitive firing from this model time course the same simplification will also be used (Gustafsson *et al.* 1978). To simulate the post-spike potential changes it is not enough to know the a.h.p. conductance changes. The computed a.h.p. curves showed an initial dip given by the current underlying the delayed depolarization. To account for this current the expression given in section VI was used. When supplied with suitable parameters this expression gives rise to a short depolarizing current pulse. It should be emphasized that the characteristics of this current were chosen to give, together with the a.h.p. conductance time course, an initial phase of the computed a.h.p. voltage similar in appearance to the a.h.p. of the real cells. The delayed

depolarization current might well be more longlasting, also affecting the shape of the initial fast conductance decay.

The a.h.p. in DSCT neurones is considerably smaller than that of motoneurones (Brook, Coombs & Eccles, 1952; Eccles, Eccles & Lundberg, 1958; Kuno, 1959). Since the input resistance is generally larger in DSCT neurones than in motoneurones (Burke & Bruggencate, 1971), the difference between these cells is even more evident if the conductance change underlying the a.h.p. is considered. There was no corresponding reduction in the a.h.p. duration in DSCT cells, the average time constant of the a.h.p. decay was within the range found for spinal motoneurones (Kernell & Sjöholm, 1972). As will be shown in a subsequent paper (Gustafsson *et al.* 1978) these a.h.p. properties are reflected in the firing behaviour of the neurones. Due to the similar a.h.p. duration, both types of neurones can fire with similar low frequency, but due to the small size of the a.h.p. the DSCT neurones will have a higher sensitivity to depolarizing current.

The peak a.h.p. amplitude was reached appreciably earlier in the DSCT neurones than in motoneurones (e.g. Eccles *et al.* 1958) which was reflected in different time courses of the computed a.h.p. conductance change. In the DSCT neurones the computed conductance displayed two phases, an initial fast decay followed by a slower exponential decline. There was no interposed plateau phase as generally found in spinal motoneurones (Baldissera & Gustafsson, 1974*a*). This difference in a.h.p. conductance time course is interesting for two reasons. First, the absence of a plateau phase in DSCT cells in spite of a well developed delayed depolarization emphasizes the dissociation between these two entities (cf. Baldissera & Gustafsson, 1974*a*). Secondly, the plateau facilitates the appearance of a short first interspike interval at the onset of rhythmic firing. This feature is well suited for the rapid development of muscle contraction (Baldissera & Parmiggiani, 1975; Burke, Rudomin & Zajac, 1976), but seemingly inappropriate for a second order sensory neurone as the DSCT cell. Although the a.h.p. mechanism is essentially the same in DSCT neurones and spinal motoneurones, the given examples clearly demonstrate a functional adaptation of the a.h.p. properties in these neurones.

We are indebted to Professor A. Lundberg for his interest and support of this study. The work was supported by the Swedish Medical Research Council (Projects no. 04767 and 00094).

## REFERENCES

BAKER, R. & PRECHT, W. (1972). Electrophysiological properties of trochlear motoneurons as revealed by IVth nerve stimulation. *Expl Brain Res.* **14**, 127–157.

BALDISSERA, F. & GUSTAFSSON, B. (1974*a*). Afterhyperpolarization conductance time course in lumbar motoneurones of the cat. *Acta physiol. scand.* **91**, 512–527.

BALDISSERA, F. & GUSTAFSSON, B. (1974*b*). Firing behaviour of a neurone model based on the afterhyperpolarization conductance time course. First interval firing. *Acta physiol. scand.* **91**, 528–544.

BALDISSERA, F. & GUSTAFSSON, B. (1974*c*). Firing behaviour of a neurone model based on the afterhyperpolarization conductance time course and algebraic summation. Adaptation and steady state firing. *Acta physiol. scand.* **92**, 27–47.

BALDISSERA, F. & PARMIGGIANI, F. (1975). Relevance of motoneuronal firing adaptation to tension development in the motor unit. *Brain Res.* **91**, 315–320.

BARRET, E. F. & BARRET, J. N. (1976). Separation of two voltage-sensitive potassium currents, and demonstration of a tetrodotoxin-resistant calcium current in frog motoneurones. *J. Physiol.* **255**, 737–775.

BROCK, L. G., COOMBS, J. S. & ECCLES, J. C. (1952). The recording of potentials from motoneurones with an intracellular electrode. *J. Physiol.* **117**, 431–460.

BURKE, R. E. & BRUGGENCATE, G. TEN (1971). Electrotonic characteristics of alpha motoneurones of varying size. *J. Physiol.* **212**, 1–20.

BURKE, R. E., RUDOMIN, P. & ZAJAC III, F. E. (1976). The effect of activation history on tension production by individual muscle units. *Brain Res.* **109**, 515–529.

COOMBS, J. S., ECCLES, J. C. & FATT, P. (1955). The electrical properties of the motoneurone membrane. *J. Physiol.* **130**, 291–325.

ECCLES, J. C. (1957). *The Physiology of Nerve Cells.* Baltimore: The Johns Hopkins Press.

ECCLES, J. C., ECCLES, R. M. & LUNDBERG, A. (1958). The action potentials of the alpha motoneurones supplying fast and slow muscles. *J. Physiol.* **142**, 275–291.

EIDE, E. (1968). Input amplifier for intracellular potential and conductance measurements. *Acta physiol. scand.* **73**, 1A.

EIDE, E., FEDINA, L., JANSEN, J., LUNDBERG, A. & VYKLICKÝ, L. (1969). Properties of Clarke's column neurones. *Acta physiol. scand.* **77**, 125–144.

GUSTAFSSON, B. (1974). Afterhyperpolarization and the control of repetitive firing in spinal neurones of the cat. *Acta physiol. scand.*, suppl. 416.

GUSTAFSSON, B., LINDSTRÖM, S. & TAKATA, M. (1971). A re-evaluation of the afterhyperpolarization mechanism in dorsal spinocerebellar tract neurons. *Brain Res.* **35**, 543–546.

GUSTAFSSON, B. & ZANGGER, P. (1974). Depression of the afterhyperpolarization in dorsal spinocerebellar tract neurones. *Brain Res.* **72**, 320–322.

GUSTAFSSON, B. & ZANGGER, P. (1978). Effect of repetitive activation on the afterhyperpolarization in dorsal spinocerebellar tract neurones. *J. Physiol.* **275**, 303–319.

GUSTAFSSON, B., LINDSTRÖM, S. & ZANGGER, P. (1978). Firing behaviour of dorsal spinocerebellar tract neurones. *J. Physiol.* **275**, 321–343.

ITO, M. & OSHIMA, T. (1962). Temporal summation of after-hyperpolarization following a motoneurone spike. *Nature, Lond.* **195**, 910–911.

KERNELL, D. (1965). The limits of firing frequency in cat lumbosacral motoneurones possessing different time course of afterhyperpolarization. *Acta physiol. scand.* **65**, 87–100.

KERNELL, D. & SJÖHOLM, H. (1972). Motoneurone models based on 'voltage clamp equations' for peripheral nerve. *Acta physiol. scand.* **86**, 546–562.

KERNELL, D. & SJÖHOLM, H. (1973). Repetitive impulse firing: comparisons between neurone models based on 'voltage clamp equations' and spinal motoneurones. *Acta physiol. scand.* **87**, 40–56.

KLEE, M. R., PIERAU, F.-K. & FABER, D. S. (1974). Temperature effects on resting potential and spike parameters of cat motoneurones. *Expl Brain Res.* **19**, 478–492.

KRNJEVIĆ, K., PUIL, E. & WERMAN, R. (1975). Evidence for $Ca^{2+}$-activated $K^+$ conductance in cat spinal motoneurons from intracellular EGTA injections. *Can. J. Physiol. Pharmac.* **53**, 1214–1218.

KUNO, M. (1959). Excitability following antidromic activation in spinal motoneurones supplying red muscles. *J. Physiol.* **149**, 374–393.

KUNO, M. & MIYAHARA, J. T. (1968). Factors responsible for multiple discharge of neurons in Clarke's column. *J. Neurophysiol.* **31**, 624–638.

KUNO, M., MIYAHARA, J. T. & WEAKLY, J. N. (1970). Post-tetanic hyperpolarization produced by an electrogenic pump in dorsal spinocerebellar tract neurones of the cat. *J. Physiol.* **210**, 839–855.

MARTIN, A. R. (1955). A further study of the statistical composition of the end-plate potential. *J. Physiol.* **130**, 114–122.

NELSON, P. G. & FRANK, K. (1967). Anomalous rectification in cat spinal motoneurons and effect of polarizing currents on excitatory postsynaptic potential. *J. Neurophysiol.* **30**, 1097–1113.

NELSON, P. G. & LUX, H. D. (1970). Some electrical measurements of motoneuron parameters. *Biophys. J.* **10**, 55–73.

RALL, W. (1960). Membrane potential transients and membrane time constant of motoneurons. *Expl Neurol.* **2**, 503–532.

TAKAHASHI, K. (1965). Slow and fast groups of pyramidal tract cells and their respective membrane properties. *J. Neurophysiol.* **28**, 908–924.